

# Octupole state properties in $^{168}\text{Er}$ and the two-neutron $\{[521 \frac{1}{2}][633 \frac{7}{2}]\}$ configurational pair

R. A. Meyer\*

*Nuclear Chemistry Division, Lawrence Livermore National Laboratory, Livermore, California 94550  
and Institut für Kernphysik, Kernforschungsanlage Jülich GmbH, D-5170 Jülich, Federal Republic of Germany*

D. R. Nethaway and A. L. Prindle

*Nuclear Chemistry Division, Lawrence Livermore National Laboratory, Livermore, California 94550*

R. P. Yaffe

*Chemistry Department, San Jose State University, San Jose, California 95114*

(Received 28 October 1986)

Detailed spectroscopy measurements have been made of the gamma rays that follow the deexcitation of  $^{168}\text{Er}$  levels populated in the electron capture decay of  $^{168}\text{Tm}$ . These results, when combined with a reanalysis of Coulomb excitation and inelastic scattering data, provide level lifetime information and support octupole-state Coriolis-coupling calculations. The  $\{[521 \frac{1}{2}][633 \frac{7}{2}]\}$  two-neutron configurational pair deexcitation rates are compared and some evidence for  $K$  mixing among the octupole bands is presented.

## I. INTRODUCTION

The  $3^-$  octupole state in  $^{168}\text{Er}$  has been shown to have a nearly pure two-neutron  $\{[521 \frac{1}{2}][633 \frac{7}{2}]\}$  configuration.<sup>1</sup> This supports the calculations of Neergaard and Vogel<sup>2</sup> (NV), who calculate that this configuration contributes to 99% of the makeup of the  $3^-$  octupole state. Also, recent neutron-capture gamma-ray completeness studies<sup>3</sup> have established all the octupole states and have given all band members below approximately 2 MeV. The relative ordering and energy of the  $K^\pi=0^-, 1^-, 2^-, 3^-$  octupole states again confirm the prior calculations of NV. Unfortunately, analysis of Coulomb excitation data misassigned the  $K$  values of  $3^-$  states, and early (d,d') studies<sup>4</sup> could not assign  $3^-$  values to weakly excited states. This has led to the suggestion that the NV calculations were not applicable to  $^{168}\text{Er}$  (Ref. 5). Here, we show that reanalysis of the Coulomb excitation data<sup>5,6</sup> in combination with the (d,d') data do support the Coriolis redistribution of  $B(E3)\uparrow$  strength in the Coulomb excitation of  $^{168}\text{Er}$ . The new  $B(E3)\uparrow$  values in combination with our measured  $E3$  branching ratios then allow us to calculate the level half-lives and determine absolute deexcitation rates for transitions from the octupole  $3^-$  band members. These transition strengths, as well as beta transition strengths, allow us to investigate the properties of the two-neutron  $\{[521 \frac{1}{2}][633 \frac{7}{2}]\}$  configurational partners and find some evidence for  $K$  mixing among the octupole bands.

The electron capture (EC) decay of 93.1 d  $^{168}\text{Tm}$  was last studied in 1969 by Keller, Zganjar, and Pinijian<sup>7</sup> and Kenealy, Funk, and Mihelich.<sup>8</sup> However, in both of those studies low-level source strength precluded detailed investigation. Here we give the results of our detailed spectroscopy studies of the decay of  $^{168}\text{Tm}$  originally performed to measure precise values for the gamma-ray abundances used in gamma-ray metrology.<sup>9</sup>

## II. EXPERIMENTAL MEASUREMENTS

In order to perform a complete set of gamma-ray measurements, we used three separate methods to produce  $^{168}\text{Tm}$  sources. In the first, an intense source of  $^{168}\text{Tm}$  was made by irradiating a thin metal foil of thulium with the maximum flux of 14.8-MeV neutrons at the Lawrence Livermore National Laboratory's (LLNL's) Insulated Core Transformer Facility for a period of  $\sim 80$  h. The metal foil was 99.9% pure thulium and was used without chemical purification.

In the second method, a sample of  $\text{Tm}_2\text{O}_3$  was irradiated with high-energy neutrons (up to 40 MeV) at the University of California, Davis, cyclotron. The  $\text{Tm}_2\text{O}_3$  was 99.9% pure. After the irradiation, the  $\text{Tm}_2\text{O}_3$  was dissolved in acid, filtered, precipitated with  $\text{NH}_4\text{OH}$ , and reignited to  $\text{Tm}_2\text{O}_3$ .

In the third method, a source of  $^{168}\text{Tm}$  was prepared by high-energy spallation of tantalum at the Los Alamos Meson Production Facility. The tantalum target was dissolved and the thulium fraction was purified by three separate elutions through cation-exchange (Dowex-50 resin) columns. This sample was then mass separated using the LLNL Nuclear Chemistry Division's isotope separator to provide an isotopically pure sample of  $^{168}\text{Tm}$ .

A period of several months was allowed to elapse between the end of each source preparation and the beginning of any spectroscopy measurements. This allowed any  $^{167}\text{Tm}$  (9.25-d half-life) that might be present to decay away.

The sources were measured on several different Ge(Li) spectrometers at source-to-detector distances ranging from 88 to 1.3 cm. During these experiments spectra were accumulated with no absorber between the source and detector as well as with a variety of absorbers. The low-intensity high-energy gamma rays present were measured by counting with 12.4 mm of lead absorber between

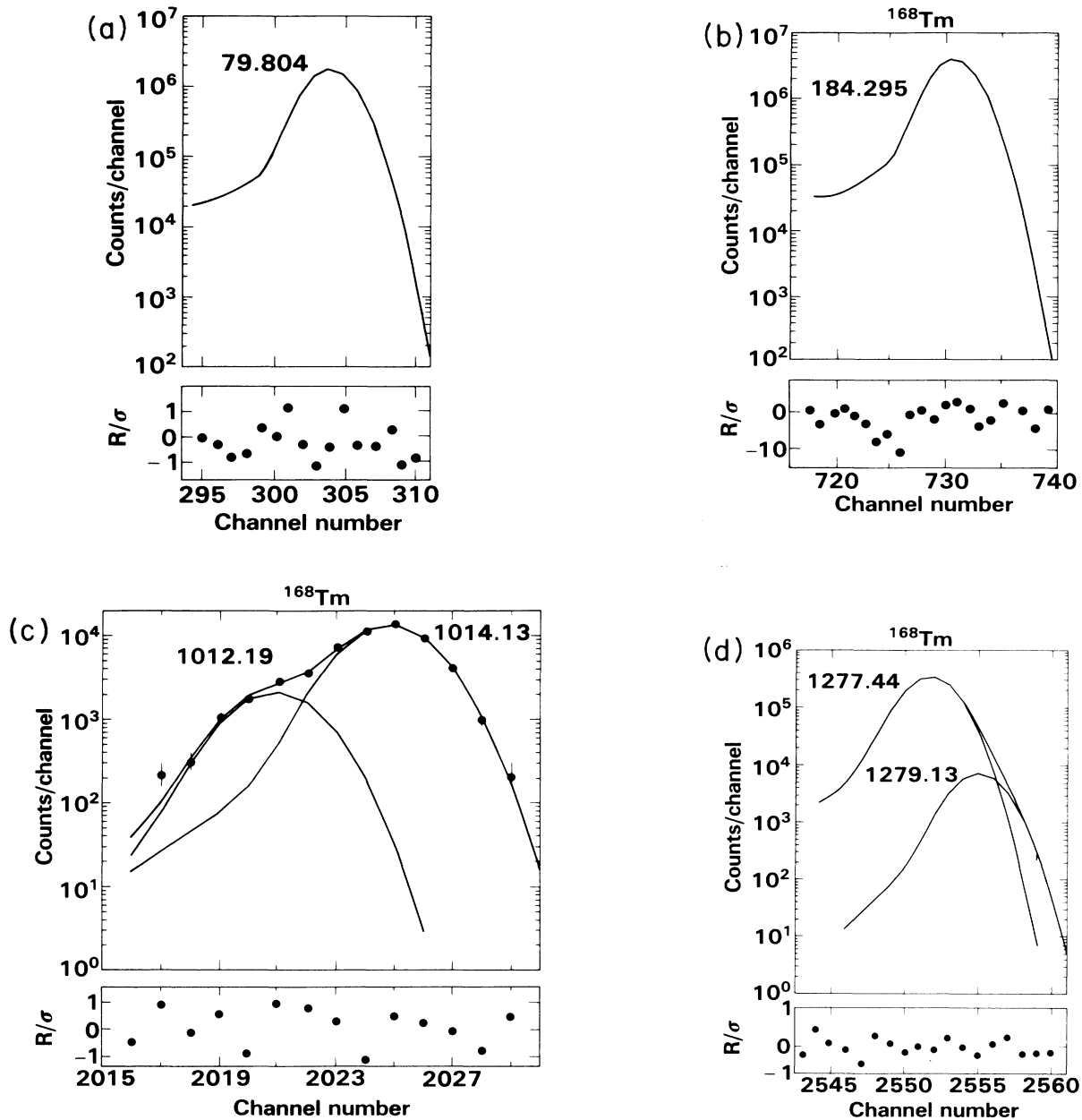


FIG. 1. Selected spectral regions from  $^{168}\text{Tm}$  spectra. The lower plot in (a)–(e) shows the residuals (in standard deviations) between the channel counts and the calculated peak shape fit. (a) Peak shape fit of the 79.804-keV photopeak. (b) Peak shape fit for the 184.295-keV photopeak. (c) Resolution of the 1012.19- and 1014.13-keV photopeaks. (d) Resolution of the 1277.44- and 1279.13-keV photopeaks. (e) Resolution of the 1489.47- and 1493.09-keV photopeaks. (f) Detection of the 511-keV annihilation radiation. (g) Detection of the 87.73-keV photopeak.

the source and detector while the source was 20 cm from the detector. This eliminated all summing peaks in the spectra. Also, because very low-intensity  $E3$  crossover transitions were to be used in the ensuing level half-life determinations, a series of measurements were made at several different source-to-detector distances on several

different detector systems. The energy calibration was performed by counting the  $^{168}\text{Tm}$  with a series of known multigamma-ray standards.<sup>10,11</sup> Also, because an accurate knowledge of the relative intensities was needed, a series of counting experiments were performed in which the  $^{168}\text{Tm}$  was measured simultaneously with standard

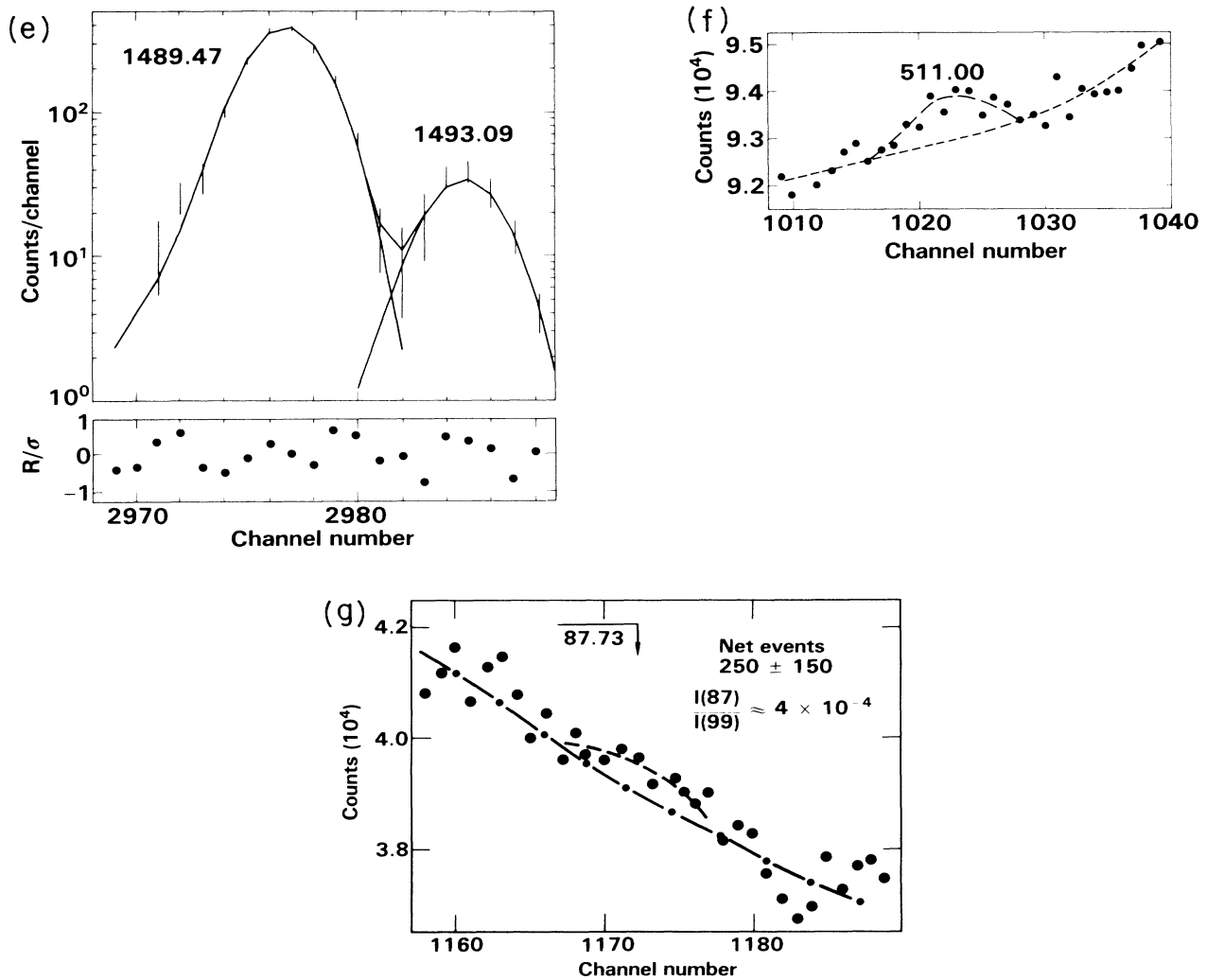


FIG. 1. (Continued).

sources such as  $^{152}\text{Eu}$  and  $^{133}\text{Ba}$ . This allowed reconfiguration of the precise shape of the detector efficiency curve at low energies at the time of measurement.

### III. RESULTS AND DECAY SCHEME

#### A. Energy and intensity values for the gamma rays

We observed several previously unobserved gamma rays in the EC and beta decay of  $^{168}\text{Tm}$ . In general, these gamma rays were detected because of better resolution and a better peak-to-Compton ratio for the detectors. In Fig. 1 we show several selected photopeaks taken from different counting conditions that illustrate our increased measurement sensitivity. Figure 1(a) and (b) show the quality of fit obtained for the 79- and 184-keV photopeaks. Figures 1(c)–(e) show the resolution of the 1012–1014, 1277–1279, and 1489–1493 photopeak doublets using the computer code GAMANAL.<sup>12</sup> The 1012-, 1279-, 1489-, and 1493-keV photopeaks were previously unknown in the

$^{168}\text{Tm}$  EC decay. The presence of any annihilation radiation in the  $^{168}\text{Tm}$  decay is of importance in determining the extent of electron capture to positron decay to the 79-keV level of  $^{168}\text{Er}$  and in determining the absolute abundances of the gamma rays. The presence of the 511-keV photopeak was observed in all spectra with a consistent intensity; a typical 511-keV spectral region is shown in Fig. 1(f). Figure 1(g) shows the spectral position of the 87.73-keV gamma ray. The presence of this photopeak, as discussed below, is evidence for the beta decay of  $^{168}\text{Tm}$  to the first  $2^+$  level of  $^{168}\text{Yb}$ .

The gamma-ray energies and intensities we measured for the decay of  $^{168}\text{Tm}$  are given in Table I. As noted in footnote c of Table I, the conversion factor for transforming the relative intensity values to gamma rays per 100 decays is 0.0522. This value was arrived at by three separate, but slightly related, methods:

- (1) Summing all transitions to the ground state (0.0522).
- (2) Accounting for all transitions populating and depopulating the 264-keV level (0.0523).

TABLE I. Energy, intensity, and assignment of gamma rays in the decay of  $^{168}\text{Tm}$  to levels of  $^{168}\text{Er}$  and  $^{168}\text{Yb}$ .

Energy <sup>a,b</sup> (keV)	Intensity <sup>c,d</sup> (Relative <sup>c</sup> )	Assignment		Energy <sup>a,b</sup> (keV)	Intensity <sup>c,d</sup> (Relative <sup>c</sup> )	Assignment	
		From	To			From	To
79.804 (2)	201 (4) <sup>e</sup>	79	g.s.	741.355 (4)	235 (1)	821	79
87.73 (2)	0.03 (2)	87(Yb)	g.s.	748.282 (7)	7.8 (1)	1569	821
99.293 (2)				812.287 <sup>h</sup>	0.2 <sup>h</sup>	1633	621
98.982 <sup>f</sup>	2.8 (4) <sup>g</sup>	1193	1094	815.989 (5)	935 (3)	895	79
99.289 <sup>f</sup>	77.7 (4) <sup>g</sup>	1094	994	821.162 (2)	220 (1)	821	g.s.
173.591 (19)	0.77 (4)	994	821	829.948 (6)	128 (1)	1094	264
184.295 (2)	333 (3)	264	79	853.468 (3)	0.63 (3)	1117	264
198.251 (2)	1000 (3)	1094	895	862.6 (3)	0.027 (15)	1411	548
221.8 (5)	0.04 (2)	1117	895	914.933 (4)	57.2 (3)	994	79
272.896 (13)	1.70 (7)	1094	821	928.916 (7)	1.17 (3)	1193	264
284.655 (14)	1.66 (8)	584	264	1012.26 (6)	0.21 (2)	1276	264
348.509 (2)	6.49 (7)	1541	1193	1014.226 (10)	1.35 (5)	1094	79
422.305 (7)	5.59 (8)	1615	1193	1025.4 (4)	0.0006 (4)	1574	548
447.501 (2)				1137.36 (15)	0.008 (4)	1217	79
445.995 <sup>f</sup>	1.4 (4)	994	548	1167.357 (6)	1.36 (3)	1431	264
447.515 <sup>f</sup>	440 (2)	1541	1094	1196.510 (52)	0.074 (9)	1276	79
497.782 (58)	0.68 (8)	1615	1117	1229.08 (11)	0.015(9)	1493	264
511 (—)	0.15 (3)	positron ann.		1277.451 (5)	30.9 (2)	1541	264
521.134 (66)	0.58 (7)	1615	1094	1279.100 (23)	0.66 (4)	1358	79
546.805 (30)	48.7 (4)	1541	994	1310.0 (3)	0.0012 (9)	1574	264
557.083 (12)	4.1 (2)	821	264	1323.909 (9)	0.40 (1)	1403	79
559.5 (4)	0.15 (5)	1653	895	1331.39 (9)	0.015 (4)	1411	79
568.8 (4)	0.11 (5)	1117	548	1351.575 (5)			
582.57 (25)	0.03 (2)	1403	821	1351.24 <sup>h</sup>	0.28 <sup>h</sup>	1431	79
620.59 (7)	0.14 (5)	1615	994	1351.542 <sup>h</sup>	1.33 (2) <sup>h</sup>	1431	79
631.705 (3)	170 (1)	895	264	1358.904 (14)	0.19 (1)	1358	g.s.
645.766 (3)				1392.209 <sup>h</sup>	< 0.0004	1656	264
644.277 <sup>f</sup>	0.23 <sup>h</sup>	1193	548	1413.35 (15)	0.008 (2)	1493	79
645.775 <sup>f</sup>	27.7 (2)	1541	895	1431.68 (38)	0.0068 (15)	1431	g.s.
673.670 (15)	3.0 (1)	1569	994	1461.750 (4)	4.54 (6)	1541	79
720.379 (4)				1489.655 (31)	0.039 (2)	1569	79
719.550 <sup>f</sup>	3.8 <sup>h</sup>	1615	895	1493.7 (2)	0.0037 (6)	1573	79
720.392 <sup>f</sup>	224	1541	821	1541.56 (3)	0.042 (2)	1541	g.s.
730.660 (4)	96.8 (4)	994	264	1553.5 (7)	0.0008 (4)	1633	79
737.7 (7)	0.2 (1)	1633	895	1569.5 (4)	0.0004 (2)	1569	g.s.

<sup>a</sup>Gamma-ray energy and intensity errors are given in parentheses.

<sup>b</sup>Where no energy value is given the energy value was taken from Ref. 3.

<sup>c</sup>Intensities given are relative to the 198-keV gamma-ray intensity being taken as 1000 units.

<sup>d</sup>Conversion from relative intensity to absolute intensity in percent is obtained by multiplying these values by 0.0522.

<sup>e</sup>In a large volume Ge(Li) or high-purity Ge detector this gamma ray may give an apparent intensity in the range from 190 to 208 units. This is due to several factors beyond the problem of correct efficiency description including summing and pulse pileup loss. Our best value comes from several measurements using different detectors and different spectrometer gains.

<sup>f</sup>Doublet.

<sup>g</sup>The intensity ratio of 1 to 28 for the intensity of the 98.982 to that of the 99.289 gamma-ray intensity was determined using a high-resolution LEPS spectrometer.

<sup>h</sup>This value was determined by using other known gamma rays from the same level and the level branching ratios as determined in the neutron-capture gamma-ray experiments of Davidson *et al.* (Ref. 3).

(3) Performing a detailed analysis for the entire decay scheme (0.0521).

#### B. Decay scheme for $^{168}\text{Tm}$ and levels of $^{168}\text{Er}$

We present the decay scheme for  $^{168}\text{Tm}$  in Fig. 2, and in Table II we give the  $\log ft$  values for the EC population of the levels. The spin and parity values for the levels are known from previous studies.<sup>13</sup> In general, the gamma-

ray energies independently determined in this work against multigamma-ray standards<sup>10,11</sup> agreed, within experimental error, with the values obtained in earlier neutron-capture gamma-ray studies. A comparison of the intensity values is given in Table III, where the most intense transition from a given level is taken as 100 arbitrary units. The branching ratios, given in columns 2 and 3, are from the work of Davidson *et al.*,<sup>3</sup> and those in column 3 labeled EC decay are the values from this work.

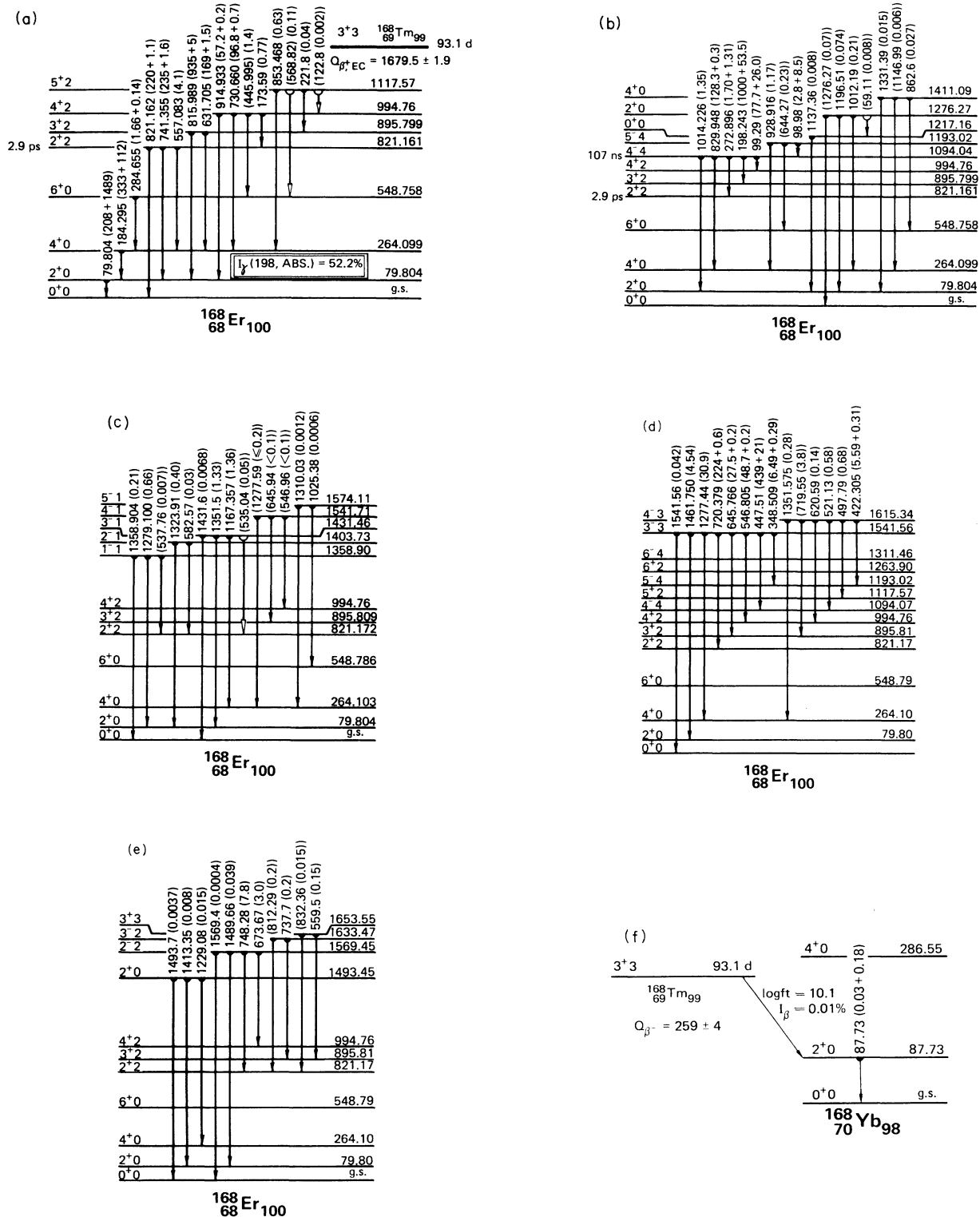


FIG. 2. Decay scheme for the decay of  $^{168}\text{Tm}$  to levels of  $^{168}\text{Er}$  and  $^{168}\text{Yb}$  [the numbers given in parentheses are relative transition intensities (gamma-ray + conversion-electron intensities) normalized to an intensity of 1000 for the 198-keV gamma-ray intensity]. (a) Population of the ground state and gamma-vibration bands. (b) Population of the two neutron  $[521 \frac{1}{2}][633 \frac{7}{2}]4^-$  at 1094.04 keV and the  $0^+$  band at 1217.16 keV. (c) Population of the  $K^\pi = 1^-$  octupole band. (d) Population of the two neutron  $[521 \frac{1}{2}][633 \frac{7}{2}]3^-$  band. (e) Population of the 1493-, 1569-, 1633-, and 1653-keV levels. (f) Population of the 87-keV level of  $^{168}\text{Yb}$ .

In general, there is good agreement between the two sets. However, the EC decay results show that in some cases, the capture gamma-ray data must contain unresolved doublets. For example, the  $E1$  transition from the  $2^-2$  band head at 1569.45 keV to the  $2^+0$  ground-state (g.s.) band member is given as 4% of level deexcitations where, in fact, the beta decay is an order of magnitude less, at 0.36%. Also, in some cases, where close lying doublets are separated in energy by less than the resolution, the values are incorrectly proportioned even though they may result from fits to more than one order of reflection in the bent-crystal work. An example of this is the partitioning of intensity between transitions arising from two close lying levels, at 1541.56 and 1541.76 keV, with  $3^-3$  and  $4^-1$  values, respectively. The EC decay populates the 1541.56-keV level intensely. If we use the extent of EC decay to other members of the  $K=1$  band and simple Alaga rules for the distribution of EC decay to other members of a band as a guide to approximating the population of the  $4^-1$  member, we find that we should expect

TABLE II. Level population and  $\log f_{n\uparrow}$  values.

Level	$I^\pi K$	Population (%)	$\log f_{\uparrow}$	$\log f_{1\uparrow}$
g.s.	$0^+0$			
79	$2^+0$	0.6 <sup>a</sup>	11.7	
264	$4^+0$	0.41	11.63	
548	$6^+0$			
821	$2^+2$	11.7	9.39	
895	$3^+2$	1.30	10.22	
994	$4^+2$	0.06	11.3	
1117	$5^+2$			
1094	$4^-4$	42.9	8.26	
1193	$5^-4$	0.005		11.9
1217	$0^+0$			
1276	$2^+0$	0.019	11.07	
1411	$4^+0$	0.0010	11.79	
1358	$1^-1$	0.040		10.20
1403	$2^-1$	0.020	10.47	(10.20) <sup>b</sup>
1431	$3^-1$	0.08	9.73	(9.38) <sup>b</sup>
1541	$4^-1$	$\leq 0.03$	$\geq 9.4$	$(\geq 8.8)$ <sup>b</sup>
1574	$5^-1$	$9.4 \times 10^{-5}$		10.9
1422	$0^+0$			
1493	$2^+0$	0.0014	11.13	
1656	$4^+0$	$< 2 \times 10^{-5}$	$> 10$	
1541	$3^-3$	41.6	6.26	
1615	$4^-3$	0.62	7.06	
1569	$2^-2$	0.57	7.80	
1633	$3^-3$	0.21	8.08	
1653	$3^+3$	0.0078	7.81	

<sup>a</sup>Average of the gamma-ray plus conversion electron intensity and that calculated from the positron intensity balance (see the text).

<sup>b</sup>This is the  $\log f_{1\uparrow}$  value if all the electron capture intensity proceeds through the unique first forbidden process.

less than 0.1 unit of gamma-ray intensity to arise from these transitions. Thus the gamma rays observed in EC decay can be taken as originating entirely from the deexcitation of the 1541.56-keV level (within experimental error). We note that further confirmation of this arises from the beta-decay studies of  $^{168}\text{Ho}$  by Tirsell and Multhau.<sup>14</sup> They find the same transition branching ratios as our values for the depopulation of the 1541.56-keV level in the decay of  $^{168}\text{Ho}$  with a ground-state spin parity of  $3^+$ .

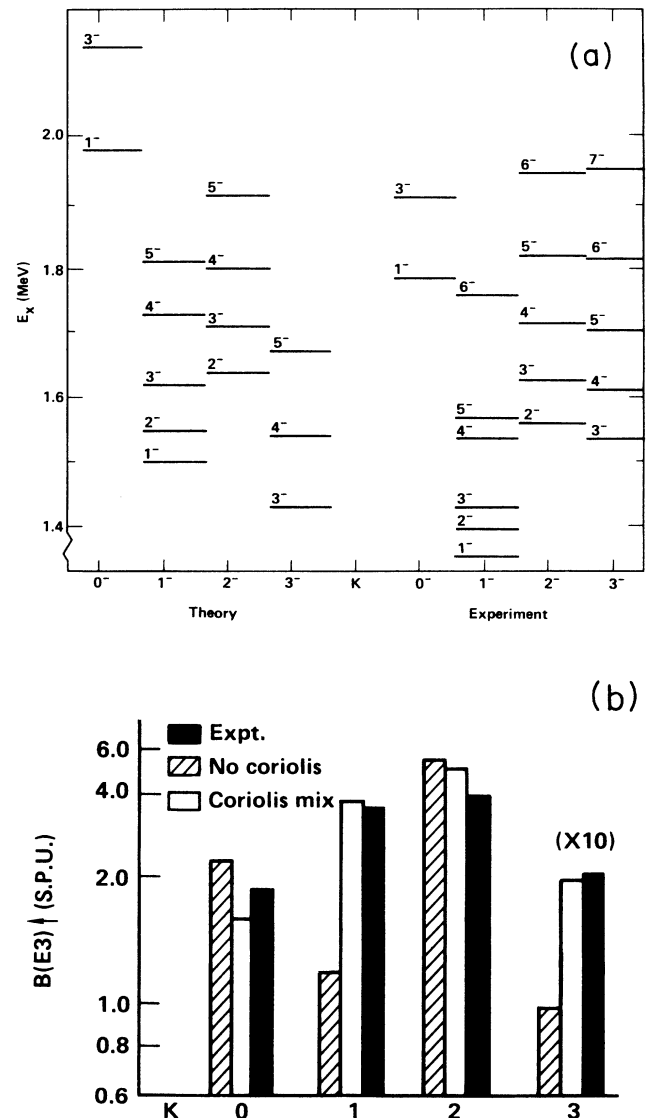


FIG. 3. (a) Comparison of the octupole band member energies calculated by Neergaard and Vogel (Ref. 2) and those known from experiments. (b) Comparison of the  $B(E3)\uparrow$  strength calculated using the model of Neergaard and Vogel (Ref. 15) (with and without Coriolis coupling) to experimental values [see the text for determination of some of the  $B(E3)\uparrow$  values].

TABLE III. Comparison of  $^{168}\text{Er}$  level branching properties determined by neutron-capture and beta decay spectroscopy.

Level and transition (keV, $I''K$ in paren.)	Origin of branching ratio		Final state ( $I''K$ )	Level and transition (keV, $I''K$ in paren.)	Origin of branching ratio		Final state ( $I''K$ )
	n capture	EC decay			n capture	EC decay	
$K''=2^+$ band (821)				$2^+0$ (1276)			
$2^+2$ (821)				1276	53(7)	a	$0^+0$
821	90(8)	93.6(4)	$0^+0$	1196	53(7)	35(41)	$2^+0$
741	100(9)	100(2)	$2^+0$	1012	100(10)	100(10)	$4^+0$
557	1.6(2)	1.74(8)	$4^+0$	455	0.91(2)		$2^+2$
$3^+2$ (895)				380	1.3(3)		$3^+2$
815	100(8)	100(2)	$2^+0$				
631	17.9(1.5)	18.1(2)	$4^+0$	$4^+0$ (1411)			
74	0.04(1)		$2^+2$	1331	77(8)	56(15)	$2^+0$
$4^+2$ (994)				1146	51(6)		$4^+0$
914	61(5)	59.1(6)	$2^+0$	862	100(10)	100(50)	$6^+0$
730	100(9)	100(2)	$4^+0$				
445	1.17(12)	1.1(1)	$6^+0$	$K''=1^-$ band (1358)			
173	0.94(11)	0.80(5)	$2^+2$	$1^-1$ (1358)			
$5^+2$ (1117)				1358	42(10)	32(2)	$0^+0$
853	100(9)	100(2)	$4^+0$	1279	100(13)	100(6)	$2^+0$
568	16(2)	17(7)	$6^+0$	537	1.1(2)		$2^+2$
221	4.1(5)	6(3)	$3^+2$				
122	0.37(6)		$4^+2$	$2^-1$ (1404)			
$K''=4^-$ band (1094)				1323	100(9)	100(3)	$2^+0$
$4^-4$ (1094)				582	30(4)	8(5)	$2^+2$
1014	0.29(5)	0.135(5)	$2^+0$	507	3.0(4)		$3^+2$
829	12.8(1.3)	12.8(1)	$4^+0$	$3^-1$ (1431)			
272	0.16(3)	0.17(1)	$2^+2$				
198	100(11)	100(2)	$3^+2$	$K''=1^-$ band (1358)			
99	7(1)	7.77(8)	$4^+2$	$4^-1$ (1542)		not observed in beta decay	
$5^-4$ (1193)				1277	100(10)	(100) <sup>b</sup>	$4^+0$
928	100(9)	100(2)	$4^+0$	645	15(1)	(32) <sup>b</sup>	$3^+2$
644	20(2)	19.7(3)	$6^+0$	546	25(5)	(27) <sup>b</sup>	$4^+2$
175	0.5(1)		$5^+2$	137	1.4(3)	(1.6) <sup>b</sup>	$2^-1$
98	180(27)	240(30)	$4^-4$	110	0.28(6)	(0.31) <sup>b</sup>	$3^-1$
$K''=0^+$ band (1217)				$5^-1$ (1574)			
$0^+0$ (1217)				1310	100(9)	100(75)	$4^+0$
1137	100(17)	100(50)	$2^+$	1025	57(7)	50(30)	$6^+0$

### C. Gamma-ray summing

Elimination of gamma-ray summing is an important factor in our spectroscopy measurements of  $^{168}\text{Tm}$  decay. For  $^{168}\text{Er}$ , we wish to use the low-intensity transitions that represent  $E3$  deexcitation of levels which are in competition with intense cascading transitions. Further, summing can lead to erroneous results when  $^{168}\text{Tm}$  decay sources are used in metrology. This is particularly true when low-intensity sources are used where the source-to-detector distance is required to be very small. That a majority of the major transitions in the  $^{168}\text{Tm}$  decay do undergo summing is illustrated in Table IV, where we compare the measurement of  $^{168}\text{Tm}$  at several source-to-detector distances. As can be seen by inspection of the last column in Table IV, only three of the gamma rays

remain at constant values when the results of the 1.3-cm counting distance are compared with those of an 88-cm counting distance. For analytical uses, we find that because of these effects it is more appropriate to calibrate the entire system of sample configuration, source-to-detector distance, and Ge(Li) detector efficiency for each measurement configuration if accurate results are required.

## IV. DISCUSSION

### A. Octupole states in $^{168}\text{Er}$

From a purely phenomenological view, the octupole states in deformed nuclei should be collective. However, Neergaard and Vogel<sup>2,15</sup> (NV) have shown that low-

TABLE III. (Continued).

Level and transition (keV, $I''K$ in paren.)	Origin of branching ratio		Final state ( $I''K$ )	Level and transition (keV, $I''K$ in paren.)	Origin of branching ratio		Final state ( $I''K$ )
	n capture	EC decay			n capture	EC decay	
$K''=3^-$ band (1542)				$K''=2^-$ band (1569)			
3-3 (1542)				2-2 (1569)			
1541	(5(1)) <sup>c</sup>	0.0096(5)	0+0	1569	(10) <sup>f</sup>	0.005(2)	0+0
1461	(3.6(9)) <sup>c</sup>	1.03(1)	2+0	1489	6(2)	0.50(3)	2+0
1277	(70(8)) <sup>d</sup>	7.04(7)	4+0	748	100(10)	100(2)	2+2
720	49(5)	51.0(5)	2+2	638	6.7(6)		4+2
645	16(3)	6.26(6)	3+2				
546	10(2)	11.1(2)	4+2	3-2 (1633)			
447	100(9)	100(2)	4-4	1553	7(2) <sup>e</sup>	0.5(2)	2+0
348	1.7(2)	1.48(3)	5-4	812	84(10)		2+2
				737	100(11)	100(50)	3+2
4-4 (1615)				638	6.7(6)		4+2
1351	(-) <sup>e</sup>	5.0(4)	4+0				
719	67(8)	(-) <sup>e</sup>	3+2	$K''=3^+$ band (1654)			
620	3.4(4)	2.5(8)	4+2	3+3 (1654)			
497	17(2)	12(1)	5+2	832	10(2)		2+2
521	12(1)	10(1)	4-4	757	0.9(2)		3+2
422	100(9)	100(2)	5-4	559	100(13)	100(30)	4-4
303	0.9(1)		6-4	229	0.26(5)		2-1
73	3.4(7)	$\leq 4$	3-3	84	0.7(2)		2-2

<sup>a</sup>Obscured by the intense 1277.451-keV transition.

<sup>b</sup>For corrected values see the text and Table III.

<sup>c</sup>A gamma ray of the correct energy is listed in the neutron-capture gamma-ray Tables of Ref. 3 but it is not assigned to this level.

<sup>d</sup>In the neutron-capture gamma-ray studies the entire intensity of this transition was assigned to the decay of the 1541.71-keV  $4^-1$  level.

<sup>e</sup>This is a doublet with the more intense component assigned elsewhere.

<sup>f</sup>This gamma ray was reported in Ref. 3 but was not assigned to any level.

TABLE IV. Comparison of intensities of selected gamma rays from the EC decay of  $^{168}\text{Tm}$  taken at source to detector distances from 1.7 to 88 cm.

Energy (keV)	Intensity <sup>a</sup>				Ratio <sup>b</sup> (%)
	Source-to-detector distance (cm)				
	88	21.7	17.7	1.3	
79	10.86 (5)	10.5 (1)	10.4 (3)	12.4 (1.2)	114
99	4.20 (2)	4.28 (3)	4.2 (2)	4.2 (1)	100
184	17.4 (2)	17.6 (2)	17.5 (5)	14.5 (3)	83
198	52.2 (5)	53.1 (5)	52.8 (5)	45.6 (3)	87
348	0.34 (1)	0.35 (2)	0.39 (4)	0.2(6)	76
422	0.29	0.30 (2)	0.34 (4)	0.23 (2)	79
446	23.0 (1)	22.6 (4)	22.7 (3)	18.0 (2)	78
547	2.54 (2)	2.53 (2)	2.53 (5)	2.25 (5)	89
631	8.84 (5)	8.71 (11)	8.81 (11)	7.20 (9)	81
645	1.45 (1)	1.49 (4)	1.5 (5)	2.69 (5)	186
720	11.9 (1)	11.8 (1)	11.9 (1)	11.2 (1)	94
731	5.05 (2)	5.00 (11)	5.0 (1)	4.38 (5)	87
741	12.27 (5)	12.27 (11)	12.5 (1)	12.17 (9)	99
748	0.41 (1)	0.42 (2)	0.41 (5)	0.39 (2)	95
816	48.8 (2)	48.7 (7)	49.0 (3)	43.8 (3)	90
821	11.48 (5)	11.5 (2)	11.5 (1)	11.6 (1)	101
830	6.68 (5)	6.8 (1)	6.76 (5)	6.9 (1)	103
915	2.99 (2)	2.98 (5)	3.01 (5)	3.16 (3)	106
1277	1.61 (1)	1.64 (3)	1.67 (5)	1.74 (2)	108
1461	0.24 (1)	0.24 (2)	0.25 (3)	0.74 (2)	308

<sup>a</sup>Gamma-ray intensity in units of gamma rays per 100 decays. Error is given in parentheses after each value.

<sup>b</sup>Ratio of intensity at a 1.30 cm counting distance to intensity at an 88 cm counting distance in percent.



energy two-quasiparticle configurations can dominate the configurational makeup of octupole states. In addition, NV have shown that the mixing brought about by the Coriolis interaction can alter the properties of the octupole states such as the  $B(E3)\uparrow$  values to members with  $3^-K$  (herein we use  $I^K$ ). Davidson and co-workers<sup>3</sup> have used neutron-capture gamma-ray techniques to establish all of the levels below approximately 2 MeV in  $^{168}\text{Er}$ . In Fig. 3(a) we compare the known octupole band members with the calculations of NV. The good agreement suggests that, for this nucleus, these calculations provide a good picture of the octupole states. Unfortunately, published Coulomb excitation data<sup>5</sup> have been used to suggest that the  $B(E3)\uparrow$  strength is in disagreement with these calculations. However, McGowan<sup>6</sup> has reanalyzed the Coulomb excitation data with the present knowledge of the location of octupole members (the presently known  $3^-1$  member at 1431 keV was originally thought to be the  $3^-0$  band member). Figure 3(b) compares the NV calculations with and without Coriolis coupling to the reanalyzed  $B(E3)\uparrow$  values taken from McGowan's reanalysis and the results of the published (d,d') experiments of Tjom and Elbek,<sup>4</sup> which have been augmented through the association of previously unidentified peaks with levels that have since been identified as octupole states. As can be seen, the Coriolis-coupled cal-

culations of NV agree with the measured  $B(E3)\uparrow$  values, particularly for the two lowest-energy octupole bands. Further support comes from recent transfer reaction studies,<sup>1,16,17</sup> which establish a  $\{[521 \frac{1}{2}][633 \frac{7}{2}]\}$  two-neutron configuration as making up  $\sim 99\%$  of the  $3^-3$  octupole band head, again consistent with the calculations of NV. Thus the octupole two-quasiparticle components calculated by NV that are given in Table V can be taken as a good indication of the major components in these bands.

### B. $\{[521 \frac{1}{2}][633 \frac{7}{2}]\}$ configurational pair properties

The  $3^-$  spin partner of the two-neutron  $\{[521 \frac{1}{2}][633 \frac{7}{2}]\}$  configuration has been determined to dominate the  $K=3$  octupole state with its band head at 1542 keV.<sup>1,16,17</sup> Using the coupling rules of Gallagher<sup>18</sup> we should expect its  $K=4$  partner to occur at a lower energy. Both  $g$ -factor<sup>19</sup> measurements and transfer reaction studies<sup>1,16,17</sup> have shown that the  $K=4$  band at 1094 keV, with a half-life of 107 ns,<sup>11</sup> has about a 70%  $\{[521 \frac{1}{2}][633 \frac{7}{2}]\}$  two-neutron component with most of the residual component (25%) coming from the  $\{[523 \frac{7}{2}][411 \frac{1}{2}]\}$  two-proton configuration. Using our intensities, earlier data, and the reanalyzed  $B(E3)\uparrow$  data, we have determined the deexcitation properties of these bandheads, which are given in Table VI.

Included in the observed deexciting transitions of the  $3^-$  bandhead are the spin-flip transitions to the band members of its  $4^-$  spin partner. As few cases have been observed,<sup>20</sup> the determination of their absolute rate is of some interest. Although no direct measurement has been made of the level lifetime, it is possible to determine the level half-life provided the  $B(E3)\uparrow$  strength and the  $E3$  deexcitation transition branching ratio are known (see Ref. 21). Using the values from our investigation, the Coulomb excitation values determined by McGowan,<sup>6</sup> and reanalysis of the work of Tjom and Elbek,<sup>4</sup> we are able to determine a half-life of 8 ps for the  $K=3$  bandhead at 1542 keV and a half-life of 41 ps for the  $3^-1$  band member at 1431 keV. The absolute transition probabilities for all observed transitions can be calculated and hindrance factors determined. The latter are given in Table

TABLE V. Octupole state components.

$K$ value <sup>a</sup>	Configuration	%
$K=0(1786/1913)$		
Proton	$[404 \frac{7}{2}][523 \frac{7}{2}]$	21
Neutron	$[514 \frac{7}{2}][633 \frac{7}{2}]$	38
	$[512 \frac{5}{2}][642 \frac{5}{2}]$	11
	$[521 \frac{1}{2}][651 \frac{1}{2}]$	6
$K=1(1358/1431)$		
Proton		<1
Neutron	$[512 \frac{5}{2}][633 \frac{7}{2}]$	89
	$[523 \frac{5}{2}][633 \frac{7}{2}]$	6
$K=2(1569/1633)$		
Proton	$[411 \frac{3}{2}][523 \frac{7}{2}]$	44
Neutron	$[521 \frac{3}{2}][633 \frac{7}{2}]$	27
	$[512 \frac{5}{2}][624 \frac{9}{2}]$	7
$K=3(1431/1542)$		
Proton	b	<1
Neutron	$[521 \frac{1}{2}][633 \frac{7}{2}]$	99

<sup>a</sup>The components listed in this table were calculated by Vogel using the model described in Ref. 2. Values in parentheses are the experimentally observed/theoretically predicted bandhead energies (in keV).

<sup>b</sup>There are no proton configurations in this band that are predicted which have over a 1% component.

		$3^+3$	g.s.
		$\{\pi[411 1/2] \nu[633 7/2]\}$	$^{168}\text{Tm}$
$3^-3$	6.26	$5^-1$	- [10.9]
0.99 $\{\nu[521 1/2] [633 7/2]\}$		$4^-1$	$\geq 9.4 [\geq 8.8]$
		$3^-1$	9.73 [9.38]
		$2^-1$	10.47 [10.18]
		$1^-1$	- [10.20]
		$\{0.89 \nu[512 5/2] [633 7/2]\}$	
		$\{0.06 \nu[523 5/2] [633 7/2]\}$	

FIG. 4. Octupole state band members in  $^{168}\text{Er}$  populated by the unique first forbidden EC decay of  $^{168}\text{Tm}$  (numbers on the right-hand side of each level is the  $\log f t$  value and number in square brackets ([ ]) is the  $\log f_1 t$  value). The Nilsson state configuration for each band (and the  $^{168}\text{Tm}$  ground state) is given below band head. The two left-hand columns represent the  $3^-$  and  $1^-$  octupole bands, while the right-hand column represents the  $^{168}\text{Tm}$  ground state that beta decays to  $^{168}\text{Er}$ .

TABLE VI. Hindrance factors<sup>a</sup> for transitions from the neutron  $[521 \frac{1}{2}][633 \frac{7}{2}]$  configurational bandheads.

To	From							
	$E1$	$4^{-4}$ $M2$	$E3$	$E1$	$3^{-3}$ $M2$	$E3$	$M1$	$E2$
$0^{+0}$						4.7		
$2^{+0}$		1.4[5]	700	2.0[7]				
$4^{+0}$	2.6[9]	[4]-[5]		2.0[6]	200-1400			
$2^{+2}$		112		4.9[4]				
$3^{+2}$	4.5[6]			3.2[5]				
$4^{+2}$	7.2[6]			1.1[5]	~20			
$4^{-4}$							67	4
$5^{-4}$								0.5

<sup>a</sup>The values are given as, for example, 1.4[5], which signifies  $1.4 \times 10^5$  hindrance over the Weisskopf estimate.

VI. Of the intraconfigurational (spin-flip) transitions, the  $3^{-3}$  to  $5^{-4}$  transition must be  $E2$ ; however, the  $3^{-3}$  to  $4^{-4}$  transition can have both  $M1$  and  $E2$  character. Iwashita<sup>22</sup> has performed directional correlation measurements for the gamma rays associated with the beta decay of  $^{168}\text{Tm}$  to  $^{168}\text{Er}$ . The  $3^{-3}$  to  $4^{-4}$  bandhead-to-bandhead transition was measured to have an 0.8%  $E2$  component, which gives an  $E2$  component that is 8 times slower than the  $3^{-3}$  to  $5^{-4}$  transition.

In general, we should expect two orders of magnitude hindrance for every unit of  $K$  change beyond that allowed by the multipolarity of a transition.<sup>23</sup> Comparison of the deexcitation properties of the configurational partners shows that the deexcitation follows this  $K$ -hindrance rule for electromagnetic transitions. The allowed  $M2$  transitions have hindrance factors of 20 and 112. This compares well with the hindrance of approximately  $10^5$  for the  $M2$  transition between the  $K=4$  bandhead and the ground-state band ( $K=0$ ) and a hindrance of approximately  $10^3$  for the  $M2$  transitions from the  $K=3$  partner to the ground-state band. A similar effect is found when the two known  $E3$  transitions are compared. The  $E3$  component of the  $4^{-4}$  to  $2^{+0}$  (g.s.b.) transition is  $\sim 200$  times slower than the  $3^{-3}$  to  $0^{+0}$  (g.s.) transition. The  $E1$  transitions exhibit a similar behavior.

The mixing of higher- $K$  two-quasiparticle states into rotational members of octupole states has been shown by Fields *et al.*<sup>24</sup> to affect the properties of octupole states in the light Er nuclei. Thus the mixing of higher  $K$ -octupole states into lower- $K$  octupole band members might be expected to occur in  $^{168}\text{Er}$  as well. Such mixing may account for the unexpected tenfold jump in EC strength within the  $K=1$  octupole band. Because there is a two-unit change in  $K$  value for EC transitions from  $3^{+3}$   $^{168}\text{Tm}$  to band members of the  $K=1$  octupole band, the EC transitions must proceed by unique first forbidden (UFF) EC decay.<sup>25</sup> The UFF transitions are governed by a single matrix element; hence they are not subject to cancellations between different EC matrix elements such as are found in ordinary first forbidden EC transitions.<sup>25</sup> As

shown in Fig. 4 (see also Table II), the UFF  $\log f_1 t$  value is 10.20 for population of the  $K=1$  bandhead. When a statistical factor for the difference in substates populated is included,<sup>25</sup> this value is consistent with the known  $\log f_1 t$  value of 9.40 for the  $^{167}\text{Tm}$  to  $^{167}\text{Er}$  UFF EC transition between the  $[411 \frac{1}{2}]$   $^{167}\text{Tm}$  ground state and the  $[521 \frac{5}{2}]$  excited state in  $^{167}\text{Tm}$  (cf. this is the basic transition from  $^{168}\text{Tm}$  with a configuration of  $\{\pi[411 \frac{1}{2}]\nu[633 \frac{7}{2}]\}$  to the  $^{168}\text{Er}$   $1^{-1}$  octupole state with an 89% two-neutron  $\{[512 \frac{5}{2}][633 \frac{7}{2}]\}$  configuration<sup>26</sup>). For pure states, only the UFF process should contribute to the population of other band members even though the spin difference would allow a first forbidden transition to occur. The high  $\log f t$  (or  $\log f_1 t$ ) value for the population of the  $2^{-1}$  member is consistent with this picture. However, if there is  $K$  mixing into a band member, then first forbidden EC transitions become possible. This may be the cause of the factor of approximately 10 increase in the EC strength to the  $3^{-1}$  member over that to the  $2^{-1}$  member. The  $K=3$  octupole band is near in energy and, as discussed above, has a nearly pure two-neutron  $\{[521 \frac{1}{2}][633 \frac{7}{2}]\}$  configuration which is populated with a  $\log f t$  of 6.26. Thus only a small admixture of the  $K=3$  band into the  $3^{-1}$  band member could account for the increase in EC population of the  $3^{-1}$  state.

#### ACKNOWLEDGMENTS

We wish to thank Prof. P. Vogel of the California Institute of Technology for providing us with his calculations of the octupole states in  $^{168}\text{Er}$  and Dr. F. K. McGowan of Oak Ridge National Laboratory for performing a reanalysis of his Coulomb excitation data. One of us (R.P.Y.) wishes to thank the Nuclear Chemistry Division of LLNL for its continuing hospitality and Associated Western Universities for their continuing support. Another of us (R.A.M.) wishes to thank Prof. O. W. B. Schult and his staff at the Institut für Kernphysik, Kernforschungsanlage (KFA) Jülich, Jülich, Federal Republic

of Germany, for their hospitality during a sabbatical stay which allowed part of this work to be completed. This work was supported, in part, by the U.S. Department of Energy under Contract No. W-7405-Eng-48; Institut für

Kernphysik II, KFA Jülich GmbH, Jülich, Federal Republic of Germany, and by the Fulbright Foundation through the Council for International Exchange of Scholars (R.A.M.).

\*Permanent address: Nuclear Chemistry Division, Lawrence Livermore National Laboratory, Livermore, CA 94550.

<sup>1</sup>D. G. Burke, B. L. W. Maddock, and W. F. Davidson, Nucl. Phys. **A442**, 424 (1985).

<sup>2</sup>K. Neergaard and P. Vogel, Nucl. Phys. **A145**, 33 (1970).

<sup>3</sup>W. F. Davidson, D. D. Warner, R. F. Casten, K. Schreckenbach, H. G. Borner, J. Simic, M. Stojanovic, M. Bogdanovic, S. Koicki, W. Gelletly, G. B. Orr, and M. L. Stelts, J. Phys. G **7**, 455 (1981); **7**, 843(E) (1981).

<sup>4</sup>P. O. Tjom and B. Elbek, Phys. **A107**, 385 (1968).

<sup>5</sup>F. K. McGowan, W. T. Miller, R. L. Robinson, P. H. Steltson, and Z. W. Grabowski, Nucl. Phys. **A297**, 51 (1978).

<sup>6</sup>F. K. McGowan, private communication.

<sup>7</sup>G. E. Keller, E. F. Zganjar, and J. J. Pinajian, Nucl. Phys. **A129**, 481 (1969).

<sup>8</sup>P. F. Kenely, E. G. Funk, and J. W. Mihelich, Nucl. Phys. **A129**, 481 (1969).

<sup>9</sup>R. A. Meyer, D. Nethaway, and A. L. Prindle, Lawrence Livermore National Laboratory, FY82 Nuclear Chemistry Division Annual Report, LLNL, 1982, p. 32.

<sup>10</sup>R. A. Meyer, *Multigamma-Ray Standards*, Lawrence Livermore National Laboratory Manual M-100, 1979.

<sup>11</sup>*Table of Isotopes*, edited by C. M. Lederer and V. Shirley, 7th ed. (Wiley, New York, 1979).

<sup>12</sup>R. Gunnink and J. B. Niday, Lawrence Livermore National

Laboratory Report UCRL-51061, 1972, Vols. I–IV.

<sup>13</sup>R. Greenwood, Nucl. Data Sheets **11**, 385 (1974).

<sup>14</sup>K. G. Tirsell and L. G. Multhauf, Phys. Rev. C **7**, 2108 (1973).

<sup>15</sup>P. Vogel, private communication.

<sup>16</sup>D. G. Burke, W. F. Davidson, J. A. Cizewski, R. E. Brown, E. R. Flynn, and J. W. Sunier, Can. J. Phys. **63**, 1309 (1985).

<sup>17</sup>D. G. Burke, B. L. W. Maddock, and W. F. Davidson, Nucl. Phys. **A442**, 424 (1985).

<sup>18</sup>C. J. Gallagher, Jr., Phys. Rev. **126**, 1525 (1962).

<sup>19</sup>A. Furusawa, M. Kanazawa, and S. Hayashibe, Phys. Rev. C **21**, 2575 (1980).

<sup>20</sup>W. Andrejtscheff, K. D. Schilling, and P. Manfrass, At. Data Nucl. Data Tables **16**, 515 (1975).

<sup>21</sup>A. Bohr and B. R. Mottelson, *Nuclear Structure, Vol I* (Benjamin, New York, 1969).

<sup>22</sup>T. Iwashita, J. Phys. Soc. Jpn. **50**, 3191 (1981).

<sup>23</sup>A. Bohr and B. R. Mottelson, *Nuclear Structure, Vol. II* (Benjamin, New York, 1975).

<sup>24</sup>C. A. Fields, K. H. Hicks, R. A. Ristinen, F. W. N. de Boer, L. K. Paker, and P. M. Walker, Phys. Rev. C **26**, 290 (1982).

<sup>25</sup>E. J. Konopinski, *The Theory of Beta Radioactivity* (Wiley/Interscience, New York, 1966).

<sup>26</sup>Z. Preibsz, D. G. Burke, and R. A. O'Neil, Nucl. Phys. **A201**, 486 (1973).